JACS
JOURNAL OF THE AMERICAN CHEMICAL SOCIETY

Communication

pubs.acs.org/JACS

A Cu^{II}_2 Paramagnetic Chemical Exchange Saturation Transfer Contrast Agent Enabled by Magnetic Exchange Coupling

Kang Du and T. David Harris*

Department of Chemistry, Northwestern University, Evanston, Illinois 60208-3113, United States

Supporting Information

ABSTRACT: The ability of magnetic exchange coupling to enable observation of paramagnetic chemical exchange saturation transfer (PARACEST) in transition metal ions with long electronic relaxation times (τ_s) is demonstrated. Metalation of the dinucleating, tetra(carboxamide) ligand HL with Cu^{2+} in the presence of pyrophosphate $(P_2O_7)^{4-}$ affords the complex $[LCu^{II}_2(P_2O_7)]^-$. Solution-phase variable-temperature magnetic susceptibility data reveal weak ferromagnetic superexchange coupling between the two $S = 1/2$ Cu^{II} centers, with a coupling constant of $J = +2.69(5)$ cm^{-1}, to give an $S = 1$ ground state. This coupling results in a sharpened NMR line width relative to a GaCu analogue, indicative of a shortening of τ_s. Presaturation of the amide protons in the Cu_2 complex at 37 °C leads to a 14% intensity decrease in the bulk water ^1H NMR signal through the CEST effect. Conversely, no CEST effect is observed in the GaCu complex. These results provide the first example of a Cu-based PARACEST magnetic resonance contrast agent and demonstrate the potential to expand the metal ion toolbox for PARACEST agents through introduction of magnetic exchange coupling.

Paramagnetic chemical exchange saturation transfer (PARACEST) magnetic resonance imaging (MRI) contrast agents represent an emerging class of molecules that offer several key advantages over conventional Gd-based proton relaxation agents, including the ability to facilitate on/off contrast switching and an inherent response to environmental parameters such as pH and temperature.[1] The mechanism through which PARACEST agents generate contrast exploits labile ligand protons within close proximity to the paramagnetic center. Here, irradiation at the resonant frequency of the exchangeable protons, along with concomitant chemical exchange of these protons with bulk water protons, induces a suppression of the bulk water signal and thus an image darkening.[2] Importantly, the paramagnetic metal imposes a large hyperfine shift on the resonant frequency of the exchangeable protons, so as to minimize interference from resonances associated with surrounding tissue and to permit rapid proton exchange. Despite the potential utility of PARACEST agents, a fundamental limitation toward their implementation arises due to proton nuclear spin relaxation enhancement induced by paramagnetic metal centers, which leads to spectral broadening and thus low sensitivity and resolution. In order to reduce proton relaxation effects, the electronic relaxation time (τ_s) of the paramagnetic metal must be minimized so that it is not resonant with the proton nuclear spin.[1]

To date, reported PARACEST agents have taken the form of non-Gd lanthanide[1,3] and first-row transition metal (Fe^{II}, Co^{II}, Ni^{II}) complexes.[4] These ions display short values of τ_s, typically in the range from 10^{-11} to 10^{-12} s, owing to low-lying excited states that arise from spin−orbit coupling and/or zero-field splitting. Lanthanide PARACEST agents are air-stable and tend to exhibit large hyperfine shifts, as high as 720 ppm vs water,[5] stemming from their large magnetic moments and strong magnetic anisotropy. Nevertheless, these agents rely on through-space pseudocontact shifts of protons, rather than through-bond contact shifts, due to the contracted 4f orbitals[1] and therefore necessitate placement of exchangeable protons within close proximity to the metal ion. Moreover, the ionic nature of lanthanides, in conjunction with their redox- and spin-state inertness, limits the design of responsive agents.[1e,3b,6] Compared to lanthanide complexes, transition metal PARACEST agents exhibit smaller hyperfine shifts, up to 135 ppm vs water,[4f] but offer more tunability through coordination and redox chemistry. Indeed, recent work has demonstrated the ability of transition metal ions with short values of τ_s to engender PARACEST agents that are stable under physiological conditions.[4c−e] Nevertheless, metal ions with large values of electronic spin and higher oxidative stability, such as $S = 5/2$ Mn^{II} or Fe^{III}, or metal ions that exhibit even more kinetically inert substitution, such as Cr^{III}, are precluded from consideration for PARACEST, as they exhibit long values of $\tau_s = 10^{-8}$−10^{-9} s and therefore induce severe NMR line broadening.[7] Taken together, these observations underscore the need for a general strategy to design transition metal-based PARACEST agents with short electronic relaxation times.

A paramagnetic metal ion displays a long τ_s when the electronic ground state is energetically well-isolated from excited states, with no significant zero-field splitting or spin−orbit coupling. A representative example is octahedral Cu^{II}, where the d^9, $S = 1/2$ electronic configuration and Jahn−Teller distortion result in a long τ_s of 10^{-8}−10^{-9} s.[7] Nevertheless, several Cu^{II}_2 complexes with weak magnetic superexchange coupling between metal centers have been shown to exhibit much shorter values, as small as $\tau_s \sim 10^{-11}$ s.[8] As the separation of ground and excited state is correlated to the magnitude of exchange constant J, the presence of weak coupling leads to a low-lying excited state that can facilitate fast electronic relaxation and therefore a short τ_s. Moreover, the $S = 1$ ground or excited state, resulting from ferro- or antiferromagnetic coupling, respectively, can possess non-

Received: March 23, 2016
Published: June 8, 2016

DOI: 10.1021/jacs.6b03060
J. Am. Chem. Soc. 2016, 138, 7804−7807

negligible zero-field splitting that further decreases τ_s and can contribute to increasing the hyperfine shift.[7] Despite the potential of magnetic exchange coupling to serve as a tool to shorten τ_s, no multinuclear transition metal complexes have been reported as PARACEST agents. Herein, we demonstrate the utility of magnetic exchange coupling to enable realization of a Cu^{II}_2 PARACEST agent.

Dinuclear Cu^{II}_2 complexes supported by a phenoxo-centered tetrapyridyl ligand have previously been shown to exhibit solubility and stability in aqueous solution and weak exchange coupling of $|J| \leq 25$ cm^{-1}.[8,9] Building from these results, we targeted the analogous tetra(carboxamide) ligand HL, with the intent that the carboxamide groups could provide CEST-active protons (see Figure 1). This ligand was synthesized through an

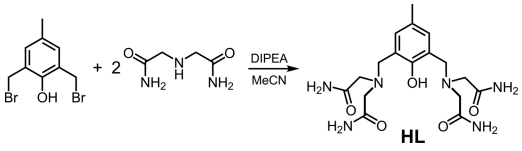

Figure 1. Synthesis of ligand HL.

S_N2 reaction between 2,2′-iminodiacetamide and 2,6-bis-(bromomethyl)-4-methylphenol (see Experimental Section and Scheme S1 in the Supporting Information). The ancillary ligand, pyrophosphate, $(P_2O_7)^{4-}$, was selected owing to its tendency to coordinate metal ions with higher thermodynamic stability than do water and coordinating anions in aqueous solution.[10] Reaction of 2 equiv of $Cu(NO_3)_2{\cdot}3H_2O$ with 1 equiv each of HL and $K_4(P_2O_7)$ in water gave a brown solution. Subsequent slow evaporation of this solution afforded brown plate-shaped crystals of $H[LCu_2(P_2O_7)]{\cdot}0.5KNO_3{\cdot}3H_2O$ (**1**). To provide a related uncoupled species for comparison to **1**, a GaCu analogue was synthesized. Here, HL was treated with 1 equiv of $Ga(NO_3)_3{\cdot}H_2O$, followed by 1 equiv each of $Cu(NO_3)_2{\cdot}3H_2O$ and $Na(H_3L'){\cdot}3H_2O$ (H_4L' = alendronic acid), to give $LGaCuL'{\cdot}4NaNO_3{\cdot}7.1EtOH$ (**2**; see Figure 2 right). Tetraanionic alendronate was employed in place of $(P_2O_7)^{4-}$ in order to impart water solubility to the neutral complex.

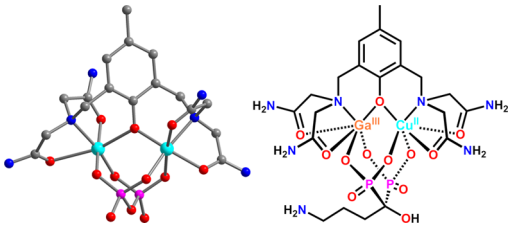

Figure 2. Left: Crystal structure of $[LCu_2(P_2O_7)]^-$, as observed in **1**. Cyan, pink, red, blue, and gray spheres represent Cu, P, O, N, and C atoms, respectively; H atoms are omitted for clarity. Right: Molecular structure of LGaCuL′, as observed in **2**.

Compound **1** crystallizes in the space group $P\bar{1}$, with an asymmetric unit that contains two nearly identical Cu_2 complexes (see Figure 2 left and Table S1). The two Cu^{II} centers of each molecule reside in distorted octahedral coordination environments, with significantly elongated Jahn–Teller axes along the O_{amide}–Cu–$O_{phenoxy}$ and $O_{phosphate}$–Cu–N_{amine} vectors. As a result, all four pendant amides are structurally inequivalent in the solid state. The pyrophosphate unit acts as a tetradentate, dinucleating ligand that coordinates the two Cu centers in a μ_2-κ^4 configuration. This binding mode presumably engenders a chelate effect of $(P_2O_7)^{4-}$ that results in preferential coordination of the Cu_2 complex over water and other anions in solution. The mean Cu···Cu distance of 3.658(1) Å is comparable to those reported for alkoxo- or phenoxo-bridged Cu^{II}_2 complexes that feature acetate bridging ligands,[7] and the mean Cu–O–Cu angle of 123.8(2)° is similar to those reported for Cu_2 complexes with weak antiferromagnetic or ferromagnetic exchange coupling.[11]

In anticipation of CEST experiments, we sought to confirm the integrity and structure of $[LCu_2(P_2O_7)]^-$ in buffered aqueous solution. Toward this end, the kinetic and thermodynamic profiles of complexation for Cu^{2+} ions by L^- and $(P_2O_7)^{4-}$ in aqueous solution were monitored by UV–vis spectroscopy. First, small aliquots of a 50 mM aqueous solution of $Cu(NO_3)_2{\cdot}3H_2O$ were titrated into a pH 7 buffer solution of 5 mM 4-(2-hydroxyethyl)-1-piperazineethanesulfonic acid (HEPES) containing 0.317 mM HL (see Figure S1). Prior to Cu addition, the spectrum of HL was characterized by one major peak at 285 nm, which we tentatively assign as a π–π^* transition. Upon Cu addition, two new features at 398 (ε = 580 M^{-1} cm^{-1}) and 726 nm (ε = 129 M^{-1} cm^{-1}) emerged, which we assign as ligand–metal charge transfer (LMCT) and d–d transitions, respectively, based on literature precedent.[8b,c] Spectral changes ceased within 3 min following each addition, suggesting relatively rapid Cu complexation by L^-. Moreover, the peak intensity at 398 nm is linearly dependent on the concentration of Cu^{2+} and reaches a maximum value upon addition of 2 equiv of Cu^{2+} (see Figure S2), suggesting the formation of a 1:2 complex of L^- and Cu^{2+} with a dissociation constant well below millimolar. The resulting species is likely the aquo adduct $[LCu_2(H_2O)_4]^{3+}$ or the μ-hydroxo adduct $[LCu_2(\mu\text{-}OH)]^{2+}$, as have been observed in related tetrapyridyl-supported Cu^{II}_2 complexes.[12]

Titration of the Cu_2 solution with a buffered pH 7 aqueous solution of $K_4(P_2O_7)$ revealed similarly rapid complexation kinetics. Here, peak maxima corresponding to the LMCT and d–d transition shifted from 398 to 432 nm (ε = 735 M^{-1} cm^{-1}) and 726 to 779 nm (ε = 104 M^{-1} cm^{-1}), respectively, with each conversion proceeding through an isosbestic point (see Figure S3). These spectral changes suggest that aquo or hydroxo ligands are displaced by $(P_2O_7)^{4-}$ ligands. In addition, the d–d transition at 779 nm lies between that of $[Cu(H_2O)_6]^{2+}$ (810 nm, ε = 12 M^{-1} cm^{-1}) and $[Cu(EDTA)]^{2-}$ (735 nm, ε = 85 M^{-1} cm^{-1}), confirming the preservation of the elongated Cu^{II} octahedral geometry in solution.[13] Fitting the absorbance data at 246 nm from titrations at lower concentration (40.2 μM) gave a dissociation constant of K_d = 9(2) μM (see Figures S3–4), confirming the high affinity of $(P_2O_7)^{4-}$. The diffuse-reflectance spectrum collected for a solid sample of **1** features peaks with maxima at 436 and 788 nm (see Figure S5), and an electrospray mass spectrum exhibits three major patterns corresponding to adducts of the anionic complex of **1** (see Figure S6). Taken together, these data lead us to conclude that the structure of $[LCu_2(P_2O_7)]^-$ determined from X-ray diffraction is preserved in aqueous HEPES solution. Finally, the spectrum of **2** exhibits similar features to that of **1** (see Figures S7–8), with the LMCT and d–d transitions at 418 nm (ε = 297 M^{-1} cm^{-1}) and 784 nm (ε = 75 M^{-1} cm^{-1}), respectively, only slightly shifted. These spectral similarities suggest that the Cu centers in **1** and **2** feature similar coordination environments in aqueous solution.

Variable-temperature dc magnetic susceptibility data were collected to determine the sign and magnitude of magnetic coupling in the Cu_2 complex. To approximate the magnetic

DOI: 10.1021/jacs.6b03060
J. Am. Chem. Soc. 2016, 138, 7804–7807

interactions in aqueous solution, magnetic data were collected on a solution of **1** in a 1:1 H_2O/glycerol mixture.[14] The corresponding plot of $\chi_M T$ vs T is shown in Figure 3. Due to

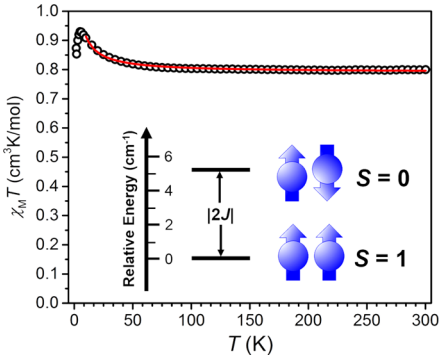

Figure 3. Variable-temperature dc magnetic susceptibility data for **1** in 1:1 H_2O/glycerol, collected under an applied field of 1 T. The red line corresponds to a fit of the data. Inset: Spin ladder and graphical representation of the energetic separation between $S = 1$ ground and $S = 0$ excited states.

the error associated with mass determination of such a small amount of solute, the number of moles of Cu_2 complex was determined by a fixed $g = 2.0629$ obtained from X-band EPR, along with the assumption that the high-temperature values of $\chi_M T$ correspond to two noninteracting $S = 1/2$ centers (see Experimental Section and Figure S10). With decreasing temperature, $\chi_M T$ remains relatively constant to ~100 K, whereupon it undergoes a gradual increase to a maximum value of $\chi_M T = 0.929$ cm^{3}K/mol at 6 K. Below 6 K, $\chi_M T$ decreases sharply to a minimum value of 0.853 cm^{3}K/mol at 2 K. The increase in $\chi_M T$ below 100 K stems from ferromagnetic coupling between the Cu^{II} ions, likely dominated by superexchange through the phenoxo bridge, to give an $S = 1$ ground state.

The data were fit in the range 10−300 K to the Van Vleck equation considering the spin Hamiltonian $\hat{H} = -2J(\hat{S}_{Cu1} \cdot \hat{S}_{Cu2})$, where $\hat{S}_{Cu1}$ and $\hat{S}_{Cu2}$ are the spin operators.[15] The fit to the data gave an exchange constant of $J = +2.69(5)$ cm^{-1}, indicating a weak ferromagnetic Cu···Cu interaction (see Figure 3). This interaction results in an energetic separation of the $S = 1$ ground state and $S = 0$ excited state of only 5.38 cm^{-1} (see Figure 3, inset), which suggests that **1** may feature a considerably shortened τ_s relative to a monocopper complex with Cu^{II} in similar coordination.

The relaxation of proton nuclear spins in **1** and **2** was probed by ^{1}H NMR to obtain a qualitative comparison of τ_s. Here, electronic spins with long values of τ_s induce a shortening of spin−lattice relaxation time (T_1) in proximal nuclear spins, which leads to a broadening of the NMR spectra. Such an analysis has been previously employed to obtain a qualitative measure for τ_s in related Cu_2 complexes.[7,8b] Importantly, the presence of similar local coordination at Cu^{II} in **1** and **2** suggests that the hyperfine shifts of analogous protons on the two complexes should be similar. In the case of **1**, the ^{1}H NMR spectrum collected for a 10 mM H_2O solution at 37 °C features three paramagnetically shifted resonances at 12, 14, and 29 ppm vs H_2O. Inversion recovery experiments of the three peaks gave values of $T_1 = 8(1)$, 13(1), and 22(4) ms, respectively (see Experimental Section and Figure S11), suggesting that the T_1 shortening of the peaks by the Cu^{II} centers is comparable for all three resonances. In addition, the peak at 29 ppm is absent in the spectrum of **1** in D_2O, indicating that this peak corresponds to the exchangeable amide protons. The presence of only one amide resonance suggests fast interchange among the four pendant arms in solution that leads to an average of four inequivalent amides. As such, the broadness of the amide resonance, compared to the other two paramagnetic peaks, is likely due to the combination of fast molecular dynamics and proton exchange, rather than relaxation induced by Cu^{II}. In contrast, an aqueous sample containing 30 mM of **2** in either D_2O or H_2O gave a spectrum that is absent of resolvable resonances in the paramagnetic region (see Figure S11), presumably due to line broadening induced by Cu^{II}. This comparison provides strong qualitative evidence that the Cu_2 complex in **1** features a shorter τ_s than does the GaCu complex in **2**, likely resulting from the presence of weak magnetic exchange coupling in **1**.[8b]

The dramatic sharpening of the NMR line widths for the Cu_2 complex relative to the GaCu analogue indicates the possibility to observe the CEST effect. We therefore collected ^{1}H NMR spectra on solutions of **1** and **2** in 50 mM HEPES buffer at pH 7 and 37 °C on an 11.75 T NMR spectrometer (see Figure 4). The

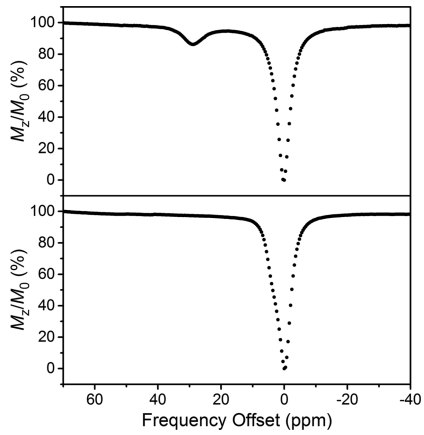

Figure 4. CEST spectra of 10 mM of **1** (top) and 30 mM of **2** (bottom) solutions in 50 mM of HEPES buffer at pH 7 and 37 °C, with a 2 s presaturation pulse of 21 μT.

resulting CEST spectra, also known as Z spectra, were constructed by plotting the intensity of the water ^{1}H NMR signal (M_Z/M_0, where M_0 and M_Z correspond to the bulk water signal before and after presaturation at a given frequency, respectively) against the presaturation frequency (i.e., frequency offset) relative to the bulk water frequency, set to 0 ppm. For **1** and **2**, complete disappearance of the water signal was observed at 0 ppm, arising from direct saturation at the water proton resonance. For **1**, in stark contrast to **2**, a peak was observed at 29 ppm corresponding to a 14% decrease in intensity of the water signal due to CEST. Although significant, the CEST effect is likely limited due to incomplete presaturation of the broad resonance of the amide protons. The presence of a slight shoulder on the water resonance in **2** likely corresponds to CEST arising from carboxamide protons coordinated to the diamagnetic Ga^{III} center. Since the T_1 of water protons can significantly influence the CEST effect,[1b] these values were measured for 20 mM solutions of **1** and **2**, in addition to pure water, as $T_1 = 352(4)$ ms, 152(1) ms, and 4.36(4) s, respectively. The lower value for **2** relative to **1** is consistent with more efficient proton relaxation stemming from a longer τ_s. For **1**, the CEST peak intensity at 25 °C decreases to 7.8%, suggesting that the exchange rate of the carboxamide protons is in the slow exchange regime

DOI: 10.1021/jacs.6b03060
J. Am. Chem. Soc. 2016, 138, 7804−7807

with respect to the saturation offset (see Figure S12). The exchange rate at 37 °C was estimated at k_{ex} = 420(20) s^{-1} by employing the omega plot method (see Figure S13),[16] and this value is comparable to those reported for mononuclear Fe-based PARACEST agents with pendant carboxamide groups.[4d] Interestingly, despite containing S = 1/2 metal centers with negligible single-ion magnetic anisotropy, **1** gives rise to a CEST peak shift and intensity that is comparable to some reported mononuclear PARACEST agents comprised of the high-spin, high-anisotropy Fe^{II} ion.[4d] In sum, these experiments demonstrate the ability of **1** to provide MR contrast through the CEST effect.

Preliminary experiments were carried out to probe the stability of **1** to reduction, pH variation, and ion substitution. The cyclic voltammogram of **1** shows a reduction wave at ca. −500 mV vs NHE (see Figure S14), suggesting that **1** would not undergo reduction under physiological conditions.[17] In addition, the UV−vis spectra of **1** confirm the integrity of $[LCu_2(P_2O_7)]^-$ in the pH range 6−8 or in the presence of excess Na_2CO_3 and NaH_2PO_4 (see Figures S15−16). However, in the presence of excess Zn^{2+} ions, the LMCT is red-shifted by 20 nm, and the d−d transition disappears (see Figure S17), suggesting the presence of Zn^{II} substitution.

The foregoing results demonstrate that the limited scope of metal ions suitable for PARACEST can be expanded through introduction of magnetic exchange coupling in multinuclear complexes. Efforts are underway to extend this initial proof-of-concept investigation to metal ions with larger values of spin and higher stability and to apply this strategy to the design of responsive PARACEST agents.

■ ASSOCIATED CONTENT

Supporting Information

The Supporting Information is available free of charge on the ACS Publications website at DOI: 10.1021/jacs.6b03060.

Experimental details and data (PDF)
Crystallographic data for **1** (CIF)

■ AUTHOR INFORMATION

Corresponding Author

*dharris@northwestern.edu

Notes

The authors declare no competing financial interest.

■ ACKNOWLEDGMENTS

This research was funded by the Chemistry of Life Processes Institute, Northwestern University, and the Air Force Research Laboratory under agreement no. FA8650-15-5518. We thank Drs. L. Liu, I.-R. Jeon, and J. M. Zadrozny for helpful discussions, Dr. Y. Zhang, Prof. J. S. Anderson, and L. M. Lilley for experimental assistance, and Prof. T. J. Meade for use of his HPLC system.

■ REFERENCES

(1) (a) Zhang, S.; Winter, P.; Wu, K.; Sherry, A. D. *J. Am. Chem. Soc.* **2001**, *123*, 1517. (b) Zhang, S.; Merritt, M.; Woessner, D. E.; Lenkinski, R. E.; Sherry, A. D. *Acc. Chem. Res.* **2003**, *36*, 783. (c) Zhou, J.; van Zijl, P. C. M. *Prog. Nucl. Magn. Reson. Spectrosc.* **2006**, *48*, 109. (d) Ali, M. M.; Liu, G.; Shah, T.; Flask, C. A.; Pagel, M. D. *Acc. Chem. Res.* **2009**, *42*, 915. (e) Viswanathan, S.; Kovacs, Z.; Green, K. N.; Ratnakar, S. J.; Sherry, A. D. *Chem. Rev.* **2010**, *110*, 2960. (f) Terreno, E.; Castelli, D. D.; Viale, A.; Aime, S. *Chem. Rev.* **2010**, *110*, 3019.

(2) Ward, K. M.; Aletras, A. H.; Balaban, R. S. *J. Magn. Reson.* **2000**, *143*, 79.

(3) Selected references: (a) Zhang, S.; Michaudet, L.; Burgess, S.; Sherry, A. D. *Angew. Chem., Int. Ed.* **2002**, *41*, 1919. (b) Aime, S.; Castelli, D. D.; Terreno, E. *Angew. Chem., Int. Ed.* **2002**, *41*, 4334. (c) Terreno, E.; Castelli, D. D.; Cravotto, G.; Milone, L.; Aime, S. *Invest. Radiol.* **2004**, *39*, 235. (d) Woods, M.; Woessner, D. E.; Zhao, P.; Pasha, A.; Yang, M.-Y.; Huang, C.-H.; Vasalitiy, O.; Morrow, J. R.; Sherry, A. D. *J. Am. Chem. Soc.* **2006**, *128*, 10155.

(4) Selected references: (a) Dorazio, S. J.; Tsitovich, P. B.; Siter, K. E.; Spernyak, J. A.; Morrow, J. R. *J. Am. Chem. Soc.* **2011**, *133*, 14154. (b) Tsitovich, P. B.; Morrow, J. R. *Inorg. Chim. Acta* **2012**, *393*, 3. (c) Olatunde, A. O.; Dorazio, S. J.; Spernyak, J. A.; Morrow, J. R. *J. Am. Chem. Soc.* **2012**, *134*, 18503. (d) Dorazio, S. J.; Morrow, J. R. *Inorg. Chem.* **2012**, *51*, 7448. (e) Dorazio, S. J.; Olatunde, A. O.; Spernyak, J. A.; Morrow, J. R. *Chem. Commun.* **2013**, *49*, 10025. (f) Tsitovich, P. B.; Spernyak, J. A.; Morrow, J. R. *Angew. Chem., Int. Ed.* **2013**, *52*, 13997. (g) Jeon, I.-R.; Park, J. G.; Haney, C. R.; Harris, T. D. *Chem. Sci.* **2014**, *5*, 2461.

(5) Woods, M.; Woessner, D. E.; Sherry, A. D. *Chem. Soc. Rev.* **2006**, *35*, 500.

(6) Selected references: (a) Zhang, S.; Trokowski, R.; Sherry, A. D. *J. Am. Chem. Soc.* **2003**, *125*, 15288. (b) Zhang, S.; Malloy, C. R.; Sherry, A. D. *J. Am. Chem. Soc.* **2005**, *127*, 17572. (c) Trokowski, R.; Ren, J.; Kálmán, F. K.; Sherry, A. D. *Angew. Chem., Int. Ed.* **2005**, *44*, 6920. (d) Que, E. L.; Chang, C. J. *J. Am. Chem. Soc.* **2006**, *128*, 15942. (e) Huang, C.-H.; Morrow, J. R. *J. Am. Chem. Soc.* **2009**, *131*, 4206. (f) Que, E. L.; Chang, C. J. *Chem. Soc. Rev.* **2010**, *39*, 51. (g) Ratnakar, S. J.; Viswanathan, S.; Kovacs, Z.; Jindal, A. K.; Green, K. N.; Sherry, A. D. *J. Am. Chem. Soc.* **2012**, *134*, 5798. (h) Hingorani, D. V.; Randtke, E. A.; Pagel, M. D. *J. Am. Chem. Soc.* **2013**, *135*, 6396. (i) Ekanger, L. A.; Ali, M. M.; Allen, M. J. *Chem. Commun.* **2014**, *50*, 14835.

(7) (a) Bertini, I.; Luchinat, C. *NMR of Paramagnetic Molecules in Biological Systems*; The Benjamin/Cummings Publishing Company, Inc.: Menlo Park, 1986. (b) Bertini, I.; Luchinat, C. *Coord. Chem. Rev.* **1996**, *150*, 1. (c) Bertini, I.; Luchinat, C.; Parigi, G. *Solution NMR of Paramagnetic Molecules: Applications to Metallobiomolecules and Models*; Elsevier Science B.V.: Amsterdam, 2001.

(8) (a) Nishida, Y.; Shimo, H.; Maehara, H.; Kida, S. *J. Chem. Soc., Dalton Trans.* **1985**, 1945. (b) Murthy, N. N.; Karlin, K. D.; Bertini, I.; Luchinat, C. *J. Am. Chem. Soc.* **1997**, *119*, 2156. (c) Siluvai, G. S.; Murthy, N. N. *Polyhedron* **2009**, *28*, 2149.

(9) These values correspond to the Hamiltonian $\hat{H} = -2J(\hat{S}_{Cu1}\cdot\hat{S}_{Cu2})$.

(10) Lee, D. H.; Im, J. H.; Son, S. U.; Chung, Y. K.; Hong, J.-I. *J. Am. Chem. Soc.* **2003**, *125*, 7752.

(11) Osório, R. E. H. M. B.; Peralta, R. A.; Bortoluzzi, A. J.; de Almeida, V. R.; Szpoganicz, B.; Fischer, F. L.; Terenzi, H.; Mangrich, A. S.; Mantovani, K. M.; Ferreira, D. E. C.; Rocha, W. R.; Haase, W.; Tomkowicz, Z.; dos Anjos, A.; Neves, A. *Inorg. Chem.* **2012**, *51*, 1569.

(12) Torelli, S.; Belle, C.; Gautier-Luneau, I.; Pierre, J. L.; Saint-Aman, E.; Latour, J. M.; Le Pape, L.; Luneau, D. *Inorg. Chem.* **2000**, *39*, 3526.

(13) Baker, A. T. *J. Chem. Educ.* **1998**, *75*, 98.

(14) Note that the peak maxima in the UV−vis spectra of **1** in H_2O and 1:1 H_2O/glycerol are identical (see Figure S9).

(15) (a) Magnetic susceptibility data were fit using the program MagProp: Tregenna-Piggott, P. L. W.; *MagProp* (part of the NIST DAVE software suite), version 2.0; NIST Center for Neutron Research: Gaithersburg, MD, 2008, http://www.ncnr.nist.gov/dave. (b) Azuah, R. T.; Kneller, L. R.; Qiu, Y. M.; Tregenna-Piggott, P. L. W.; Brown, C. M.; Copley, J. R. D.; Dimeoo, R. M. *J. Res. Natl. Inst. Stand. Technol.* **2009**, *114*, 341.

(16) Dixon, W. T.; Ren, J.; Lubag, A. J. M.; Ratnakar, J.; Vinogradov, E.; Hancu, I.; Lenkinski, R. E.; Sherry, A. D. *Magn. Reson. Med.* **2010**, *63*, 625.

(17) Tsitovich, P. B.; Burns, P. J.; McKay, A. M.; Morrow, J. R. *J. Inorg. Biochem.* **2014**, *133*, 143.

DOI: 10.1021/jacs.6b03060
J. Am. Chem. Soc. 2016, 138, 7804−7807